Auto-tracking Wireless Power Transfer System with Focused-Beam Phased Array

Bo Yang, *member, IEEE*, Tomohiko Mitani, *Member, IEEE*, and Naoki Shinohara, *Senior Member, IEEE*

***Abstract*—This research used image recognition and beam forming technology to build a phased array with target tracking and transmitting the microwaves with a focused beam. The coordinate position of the target is obtained from the image recognition module and converted into phase information for the phased array. This system was constructed by a 1 × 4 5.764 GHz phased array with four 4-bit phase shifters. The phase shifters created a focused beam, which requires not only the target's direction angle but also the transmission distance. The target position as well as direction and distance information were gathered using image recognition. The tracking beam method was evaluated by simulation and actual measurement. The results showed that the focused beam can always be formed in real-time to track the target. The transfer efficiency of the focused beam was improved higher than that of uniform phase beam within a distance of 50 cm. The automatic tracking power transmission system has a response time of about 100 ms.**

***Index Terms*—beam forming, image recognition, phased array, tracking wireless power transmission, wireless power transfer**

I. Introduction

Wireless power transfer (WPT) technology, such as Qi charging for mobile phones [1], [2], near-field communication technology for low-power devices [3], [4] and radio-frequency identification technology [5], [6], is becoming more practical. The power transmission distance of microwave WPT technologies is much longer than that of other WPT technologies [7], such as electromagnetic induction technology [8] and magnetic resonance wireless technology [9]. The Japanese government has opened three frequency bands with a maximum power of 32 W for 5.7 GHz band microwave WPT application [10] based on the advantages of long-distance transmission of microwave wireless charging technology, the broad application prospects of Internet of Things (IoT) devices, and low-power electronic products. This development will significantly promote the commercialization of microwave WPT technology. The specific parameters of the Japanese microwave WPT regulations are given in [11].

The microwave WPT technology can construct a ubiquitous charging environment. However, the nondirectional microwaves will cause electromagnetic pollution and energy waste. The microwave tracking WPT technology is an ideal realization method. The target detection method and beam direction control method are required for the tracking and WPT charging of a moving target. There are numerous target detection methods, namely, (1) satellite positioning, such as Global Positioning System (GPS) [12]; (2) radar positioning [13]; (3) radio signal location, such as Wi-Fi round trip time (RTT) [14], ultra-wideband (UWB) [15], Bluetooth Low Energy (BLE) [16], and 5G [17]; (4) acoustic localization [18]; (5) optical positioning [19]; others [20]. There are beam forming systems using a phased array system or mechanical scan type by a motor for the beam direction control method.

The mainstream tracking WPT system uses the retrodirective technology [21]–[23]. The retrodirective technology can be described as follows: the target receiver sends a pilot signal, the transmitter identifies the direction of the target from the pilot signal, then the transmitter sends the microwave beam toward the target's direction. JAXA developed a solid-state 5.8 GHz phased array WPT microwave using the retrodirective technology for charging a flying drone within a 10 m radius [21]. The phased array controlled the microwave beam to the drone. As the drone moves, the phase of the received pilot signal changes, which is related to the phase of the transmitter antenna. The microwave beam was then renewed in real-time by the phased array so that the beam pointed toward the drone. In the receive-transmit share antenna system, the phase of the pilot signal is exactly opposite to that of the transmission signal in array element antenna, which is in a conjugate relationship.

The disadvantage of retrodirective technology is that the receiver must first use energy to send a pilot signal. It is difficult to apply in scenarios, such as IoT devices without batteries or mobile phones without electricity. There are also related studies that use the second harmonic reflected wave as a pilot signal to achieve automatic tracking [22]. However, the reflected wave technology must avoid the power amplifier's second harmonic interference at the transmitting end. Furthermore, optical positioning technology is a straightforward solution to the target batteryless problem. In 1992, a batteryless airplane experiment called the MILAX was developed [24]. The microwave beam tracking was directed toward the airplane using a computer and position data from

Manuscript received July 29, 2022, revised October 17 2022; accepted October 23, 2022. This work was supported by the Microwave Energy Transmission Laboratory (METLAB), Research Institute for Sustainable Humanosphere, Kyoto University and National Institute of Information and Communications Technology (NICT), JAPAN (Grant Number 02401). (*Corresponding author:Bo Yang.*)

Bo Yang, Tomohiko Mitani, and Naoki Shinohara are with the Research Institute for Sustainable Humanosphere, Kyoto University, Uji 611-0011, Japan (e-mail: yang_bo@rish.kyoto-u.ac.jp; mitani@rish.kyoto-u.ac.jp; shino@rish.kyoto-u.ac.jp).

two charge-coupled device cameras. At that time, the image recognition was the only recognition of the target direction, but not the target distance, which is the necessary information for setting the near-field beam. With the rapid development of image recognition technology, especially the popularization of deep learning-based image technology, recognizing the location of the target has become very simple and inexpensive, and the distance can be converted using the size of the target object.

In this study, a phased array system for automatic tracking and power transmission in the 5.7 GHz band is developed in accordance with the Japanese WPT regulations. The target position in terms of direction and distance was estimated using image recognition technology. The tracking beam of the phased array tracked the target in both the direction and angle in real-time. Additionally, the identification principle of the target position, phase control method of the beam direction, and focused beam optimization are discussed. This method was evaluated by simulation and actual measurement. The evaluation results showed that the focused beam can always be formed to track the target in real-time.

II. Theory of the Tracking WPT System and Focused Beam

The transmitter of tracking WPT technology consists of two parts, the receiver target position recognition and the microwave power beamforming. In terms of position recognition, an image recognition module (camera) can detect the receiver target position and size information, such as the *X-axis* coordinate, *Y-axis* coordinate *X_size*, and *Y_size*. Here, *X_size* and *Y_size* are the size of the target on the X-axis and Y-axis, respectively. The distance *Z* between the camera and the target is inversely proportional to the size of the target in the camera. Therefore, the target size *X_size* or *Y_size* can be used to calculate the distance *Z* which is the *Z-axis* coordinate of the target. If we set the target real size *a* mapping on the camera size as *A'_size* with a 1 m distance, *A_size* with *Z* m distance and the focal length of the camera as *L*, as shown in Fig. 1, the relation equation can be written as follows:

$$a/A'\_size = 1/L. \tag{1}$$

$$a/A\_size = Z/L. \tag{2}$$

Combining (1) and (2), the distance Z can be described as (3).

$$Z = A'\_size/A\_size. \tag{3}$$

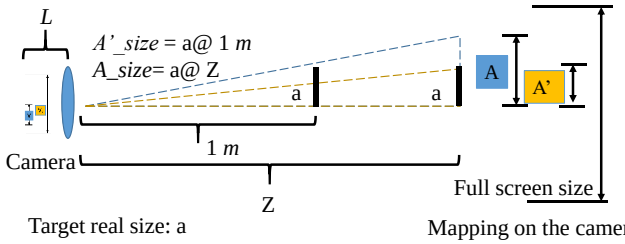

Fig. 1 Diagram of the relationship between camera size and target distance.

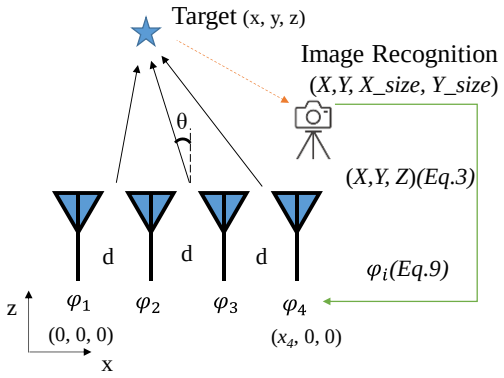

Fig. 2 Diagram of the tracking wireless power transfer system by 1 D array.

The measurement of a 6 cm target with a 1 m distance from the image recognition module (Huskeylens SEN0305) to the target, shows that the *A'_size* value was 20. The target size *A_size* in the image recognition can be converted to the target distance *Z-axis* coordinate. So far, the image recognition module can provide the coordinates (*X*, *Y*, *Z*) of the receiver target.

In a one-dimensional (1 D) array system (here, set the y = 0, the coordinate of the first antenna element as the coordinate origin), as shown in Fig. 2, the target direction angle θ can be calculated by $\tan\theta = X/Z$. When in far field area (Z >> d), the phase difference $\Delta\varphi$ between array antenna elements is shown in (4).

$$\Delta\varphi = 2\pi d \sin\theta/\lambda. \tag{4}$$

Where d denotes the spacing of the array antennas; λ is the wavelength of the microwave. All the adjacent antennas can be set with the same phase difference $\Delta\varphi$. The phase φ_i of the *N* array antenna can be described as (5) and (6).

$$\varphi_i = \varphi_{(i-1)} + \Delta\varphi. \tag{5}$$

$$\varphi_i = \varphi_{(1)} + (i-1)\Delta\varphi. \tag{6}$$

When the WPT distance is close, as shown in Fig. 2, the target angle θ with each antenna will be different, and the phase difference should be renewed as $\Delta\varphi_i$. The phase should be calculated in the near field for the optimization of beam. Here the target angle θ_i with antenna *i* is described as (7).

$$\tan\theta_i = (x_i - X)/(z_i - Z). \tag{7}$$

φ_i can be calculated by (4), (5) and (7). The phase φ_i in the near field can be described as (8).

$$\varphi_i = 2\pi\sqrt{(x_i - X)^2 + (z_i - Z)^2}/\lambda. \tag{8}$$

In Eq. (8), (x_i, z_i) are the coordinates of the antenna element of the phased array, where x_i is $(i-1)d$, and z_i is 0. Note that the phase shifter in the phased array system, such as the delay line, should have its φ_i value set to $-\varphi_i$. To summaries, φ_i can be rewritten as (9) using only the image recognition data:

$$\varphi_i = -2\pi\sqrt{((i-1)d - X)^2 + (20/X\_size)^2}/\lambda\,. \quad (9)$$

The phased array can form a focused beam toward the target by adjusting the phase φ_i of the antennas.

III. Design of the Tracking Phased Array

Fig. 3 shows the design of the auto-tracking WPT system. The data of the image recognition module (Huskeylens SEN0305) were transmitted to the LabVIEW program through an MCU board (Arduino Mega 2560). According to the principle described in Sec. II, the LabVIEW program converted the phase information into bit codes. Then, the bit codes were sent to the four 4-bit digital phase shifters α (Arumo Tech, FS00T1891) with a control accuracy of 22.5° via the digital unit (NI 9263). There are four mechanical type phase shifters β that were used to adjust the phase difference between the 4-way sub phased arrays. Each phase shifter was connected to a single subarray antenna, which used a 2 × 8 patch antenna. Fig. 4 shows the photos of the phased array system parts. The voltage control oscillator (VCO) in the phased array output 5.764-GHz signal, and the power is adjusted through the power amplifiers, and the output of each subarray can reach a maximum power of 8 W. The subarray antenna gain was designed at 19 dBi, and the composite gain is less than 25 dBi, with a main lobe angle of less than ±10° to meet the WPT regulations requirements [11].

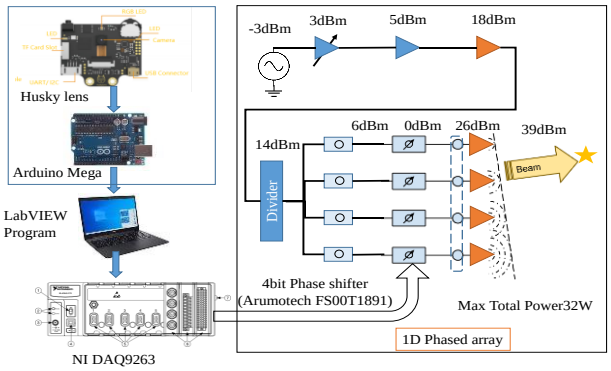

Fig. 3 Schematic diagram of the tracking wireless power transfer system.

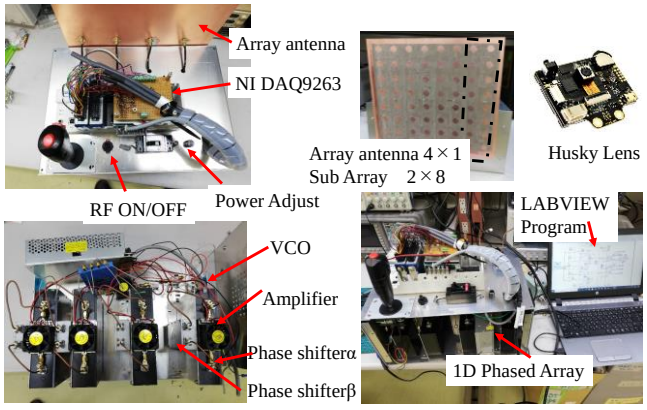

Fig. 4 Photos of the tracking phased array system.

A. Design of the subarray antenna

The tracking phased array uses four subarray antennas. Each subarray is a 2 × 8 patch antenna with a length of 81mm × 323mm, and a spacing of 0.8 wavelengths. The subarray antenna design uses equal amplitude and phase distribution with 4-level 2-divider microstrip lines. The length of the microstrip line design was adjusted using CST Studio software to achieve the antenna spacing (0.8 wavelengths) and equal phase distribution. Fig. 5 shows the design of the subarray antenna on right-handed circularly polarized. Fig. 6 shows the reflection coefficients of the four subarray antennas. The reflection values of four subarray antennas at 5.764 GHz are −19.39, −23.45, −20.03, and −17.90 dB, respectively. Each patch antenna radiates in the same phase and is connected to the center of the antenna with 16 distribution lines after being powered by a back plug-in terminal. Fig. 7 shows the beam pattern simulation result of the subarray antenna in the horizontal (phi=90°) and vertical (phi=0°) direction. The combined beam pattern of the 1 × 4 phased array is measured when the phase difference between the adjacent subarray antennas is 0°, ±22.5°, ±45°, ±67.5°, and ±90°, respectively. The main lobe beam is shifted 8.5° at 90° phase difference (8.98° by calculating equation (4)). Fig. 8 shows the shifted beam pattern.

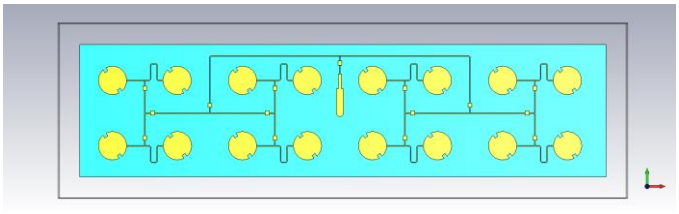

Fig. 5 Design of the subarray antenna.

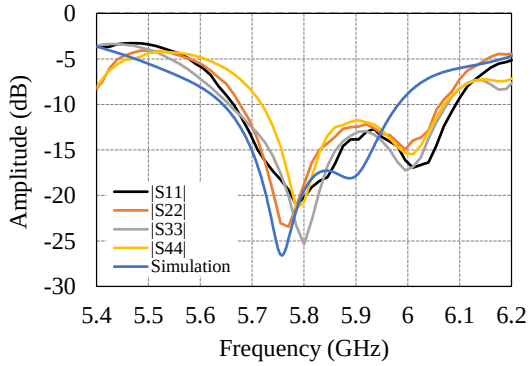

Fig. 6 Measurement and simulation result of the reflection coefficient.

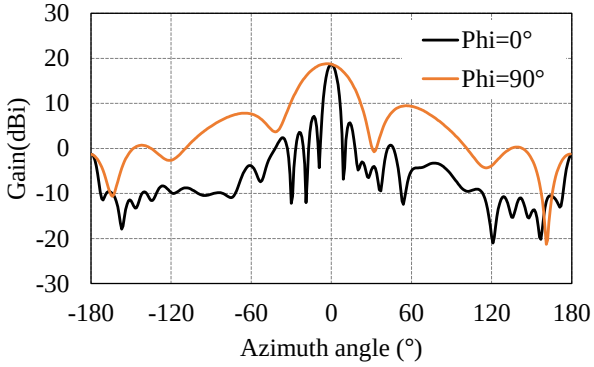

Fig. 7 Simulation results of the beam pattern of the subarray antenna.

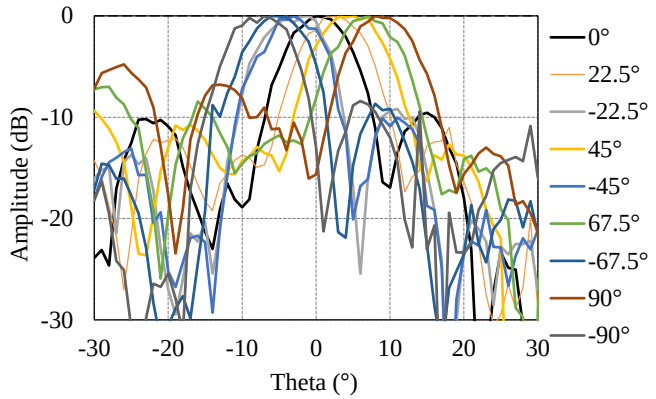

Fig. 8 Combined beam pattern of the subarray antenna with beam forming on the horizontal axis.

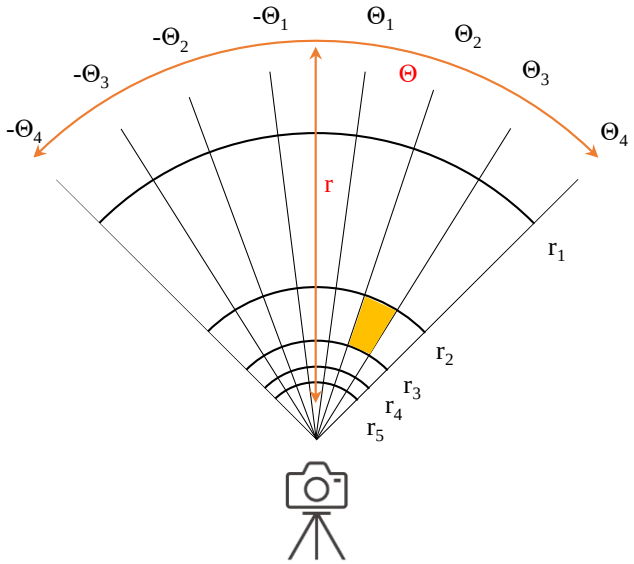

Fig.9 Division of wireless power transfer working area.

B. *Tracking program*

As described by Eq. (9) in Sec. II, the phase setting of each subarray can be calculated. However, the resolution degree of the phase shifter is limited and should be determined by the approximation. This system employs 4-bit digital phase shifters with the control accuracy of 22.5°. Here, based on the beam's accuracy, the WPT area is divided into seven angle working areas, as shown in Fig. 9. The working area is divided into six distances to achieve the higher transmission efficiency in the near-field beam. The working area corresponding to the target position is determined using the camera's position information, and the optimizer beam phase of the working area is adjusted to the phase shifter. This method can reduce computation time more than the beam phase computation. The division of the working area angle Θ_i is divided on basis of the mean value of the two beams angles θ_i, as shown in (10).

$$\Theta_i = (\theta_{i-1} + \theta_i)/2. \tag{10}$$

Where θ_0 equals 0°. The results of Θ_1 to Θ_4 is calculated in Table I.

The WPT working area ranges from $-\Theta_4$ to Θ_4. When the target position is outside this area, the transmission power is turned off.

TABLE I. DIVISION OF THE WORKING AREA IN ANGLE.

	1	2	3	4
Phase difference $\Delta\varphi$	22.5°	45°	67.5°	90°
Beam angle θ_i	2.24°	4.48°	6.71°	8.98°
Working area Θ_i	1.12°	3.35°	5.59°	7.84°

TABLE II. DIVISION OF THE WORKING AREA IN DISTANCE (m).

	1	2	3	4	5
Phase difference $\Delta\varphi$	22.5°	45°	67.5°	90°	112.5°
Focused beam L_i	2.13	1.06	0.71	0.53	0.42
Working area r_i	3.20	1.60	0.86	0.63	0.47

A near-field focused beam with different phases at different distances outperforms a uniform phase beam. A focused beam is formed in this 1 × 4 array, while the phase of the side subarrays is ahead of the phase of the center subarrays. Using Eq. (8), the focus of the beam is calculated as shown in Table II. The division method for the working area in distance is shown in (11), which is analogous to the working area in angle.

$$r_i = (L_{i-1} + L_i)/2. \tag{11}$$

where L_0 is the mean of the subarray antennas in the same phase, and the focus is infinitely large. In this system, r_1 is set to $L_1 + (L_1 - L_2)$. The tracking control method is determining the working area corresponding to the target position. For example, the image recognition module provides the coordinates (X, Y, Z) of the receiver target in the yellow working area $\Theta_2\Theta_3 r_2 r_3$ in Fig.9. The optimizer phase is coordinated ($L_2\cos\Theta_2$, $L_2\sin\Theta_2$, L_2), which is calculated in advance, the phase data [φ_i] is simply called here. Furthermore, Fig. 10 shows the simulation result of the power distribution in the working area r_5 ($z < r_5 = 0.47$ m). The power of the focused beam is more concentrated than that of the uniform phase beam.

The flowchart in Fig. 11 provides an overview of the tracking phased array control method. The image recognition module outputs target information (X, Y, *X_size*, *Y_size*) to the MCU board. The target size *X_size* is then converted to the transmission distance (Z) by the MCU board. The MCU board sends the target coordinates (X, Y, Z) to the PC LabVIEW program, which identifies the working area corresponding to the coordinates and sets the working area phase [φ_i] to the phase shifters. If the target is lost or moves outside the working area, or if software errors occur during this process, the power supply will be turned off. People are not permitted in the transmission working area under the Japanese WPT regulations, so a biological infrared detection sensor can be used to control the power supply.

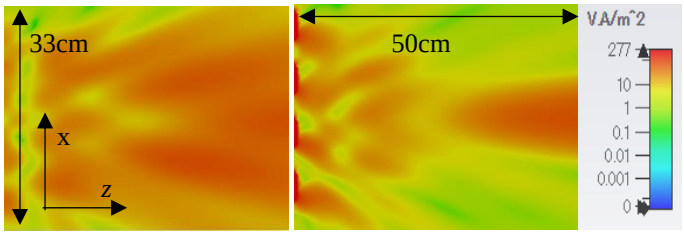

Fig. 10 Simulation results of the uniform phase beam (left) and focused beam (right).

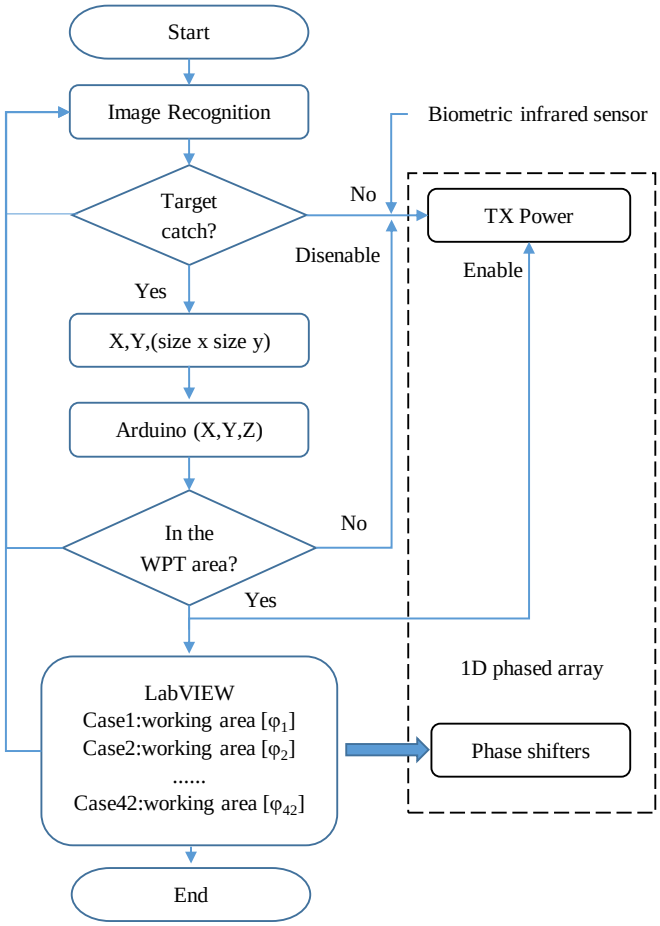

Fig.11 Flowchart of the tracking phased array control system.

IV. Demonstration Tracking WPT Experiment

The initial configuration of the phased array includes adjusting the maximum output power, output frequency and phase reset. The signal generator in the phased array is a VCO module with an integrated phase-locked loop (Maxim integrated, MAX2871), as shown in Figs. 3 and 4. The VCO module output a variable amplifier that controls the total output power of the phased array less than 32 W at 5.764 GHz, which is one frequency point specified in the Japanese WPT regulations. Phase shifters α, which are used for beamforming, are first set to 0° since the 1 × 4 phased array requires each port of the subarray to operate in the same phase. Four mechanical type phase shifters β were used to adjust all subarray antenna ports working in the same phase.

A. Tracking the WPT demonstration experiment

The control program was set up based on the instructions in the previous section. A tracking WPT demonstration experiment was constructed, as shown in Fig. 12. An LED rectifier array exists that can rectify the microwave power to dc power for supplying the LED. It was placed 1.5 m in front of the phased array to show the microwave beam. The phased array then begins to work in accordance with the flow chart in Fig. 11 after the image recognition module has selected its target. The beam followed the target as it approached the LED rectifier array, as shown in Fig. 12. The transmission power would turn off when the target was far away from the work area. The LabVIEW program shows that the period from target recognition to phase changing, which controls beam tracking, is about 100 ms. The tracking response time can also be measured using a rectenna circuit that outputs dc power to the oscilloscope. Moving the target (rectenna circuit) causes the dc output voltage to drop and then return to its original level by the tracking beam, the dropped time being the tracking response time.

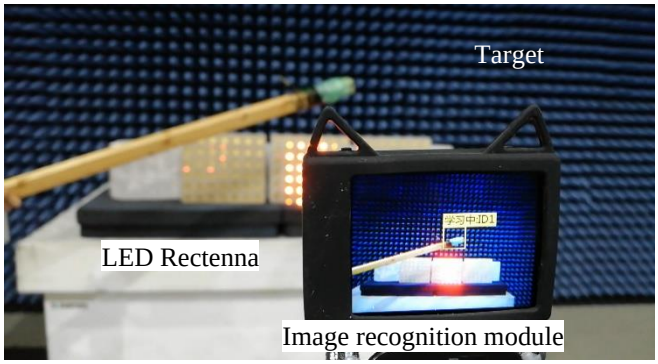

Fig. 12 Demonstration experiment of tracking wireless power transfer.

B. Tracking beam measurement experiment and beam optimization

Fig. 13 shows the measurement of the phased array beam pattern in the far field. The phased array was set in the center of the turntable with a 3 m diameter. The receiving antenna was a spiral antenna (ETS Lindgren, 3102L) located outside the turntable and set as the target for the image recognition module. The beam pattern of the phased array with tracking beam and uniform phase beam were measured, as shown in Fig. 14. The transmission efficiency of the tracking beam was improved from ±5° to ±10° as a result of these beam patterns. When the transmission beam angle was exceeded 10°, the target was deemed to be outside the working area, and the transmission power was turned off.

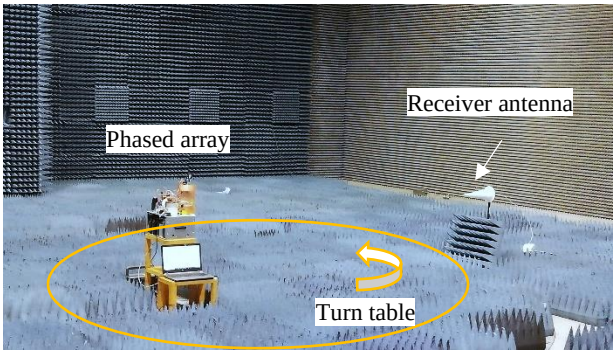

Fig. 13 Measuring the beam pattern in far field.

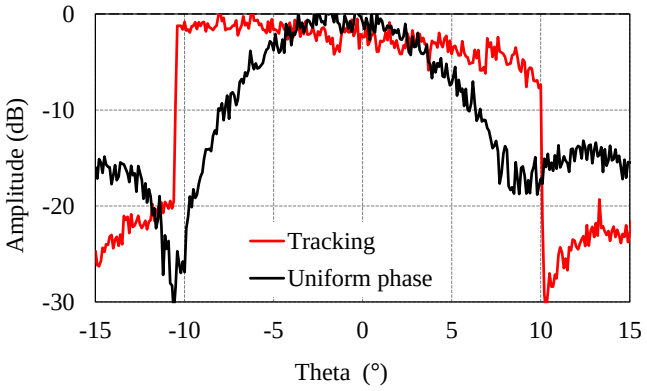

Fig. 14 Beam pattern of the tracking beam and uniform

Fig. 15 shows the measurement of the phased array beam in the near field. The X-axis and Y-axis of the waveguide probe (WR-187) were scanned to detect the E-filed amplitude of the microwave signal. The phased array was placed in the scanning center of the waveguide probe, and the antenna was parallel to the scanning plane. The width of the scan was twice that of the array antenna (13 wavelengths). The distance between the array antenna and the waveguide probe was at the beam focusing (z = *Li:* 0.42, 0.53, 0.71, 1.06 and 2.13 m), which corresponded to the optimizer beam in the working area r_1 to r_5. In the image recognition module, the target was set on the waveguide probe. Fig. 16 shows the measurement results of the beam power distribution in the near field. The power distribution of the tracking beam is more concentrated on the *X*-axis than that of the uniform phase beam.

Then, the transmission efficiency of the tracking focused beam was measured at various transmission distances. Fig. 17 shows the layout of the measurement. A sliding rail was set in front of the phased array, perpendicular to the array antenna. A receiving antenna was set on the sliding rail to measure the receiving power. This study mainly evaluates the effect of the focused beam of the transmitter on the transmission efficiency; therefore, a receiving antenna with a low gain is only practical for measurement. The receiving antenna was connected to a power meter (Agilent, N1914A) to track the received power. The target on the image recognition module is also set on the receiver antenna. The program changed the beam at various distances according to Eq. (11). Each subarray antenna of the phased array produced 8 W of microwave power. Fig. 18 shows the receiving power of the tracking-focused beam and uniform

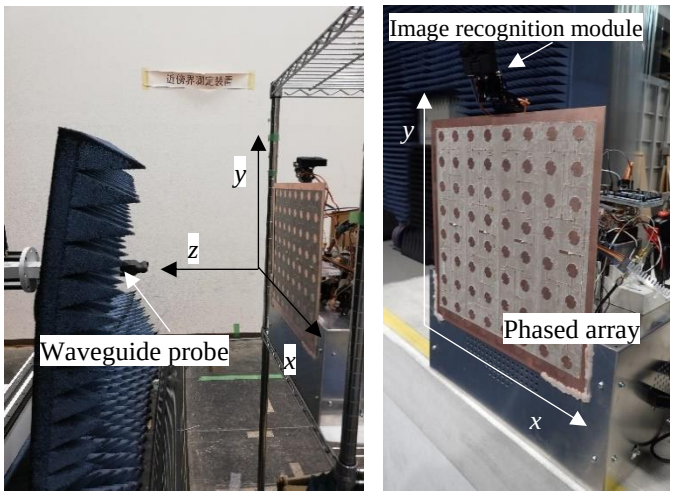

Fig. 15 Measurement of the phased array beam in the near field.

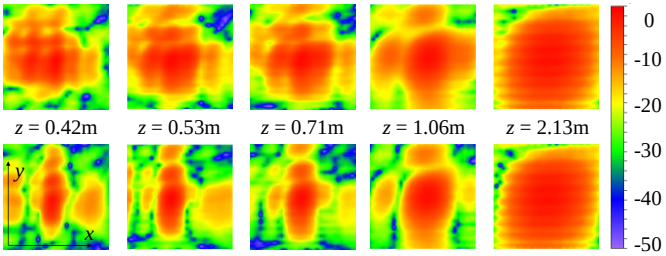

Fig. 16 Measurement of the power distribution with distance in near field. (Upper: uniform phased beam, lower: tracking beam)

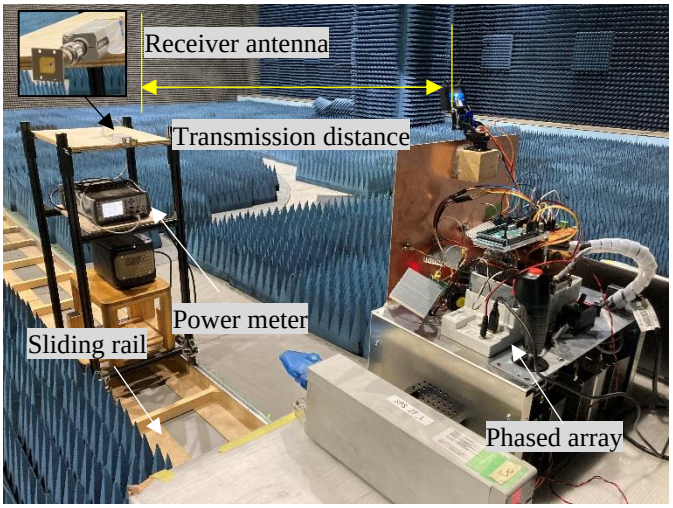

Fig. 17 Measured the beam transmission efficiency with distance.

phase beams with distances. At distances under 50 cm (about 10 wavelengths, 1.5 times array antenna size), the receiving power of the tracking beam was clearly greater than that of the uniform phase beam. At distances longer than 100 cm (about 20 wavelengths), the receiving power of the uniform phase beam isn't significantly different from that of the tracking beam. It is considered that for a transmitting antenna with a side length of 6.5 wavelengths, the focused beam can significantly improve the transmission efficiency under 20 wavelength distance approximately.

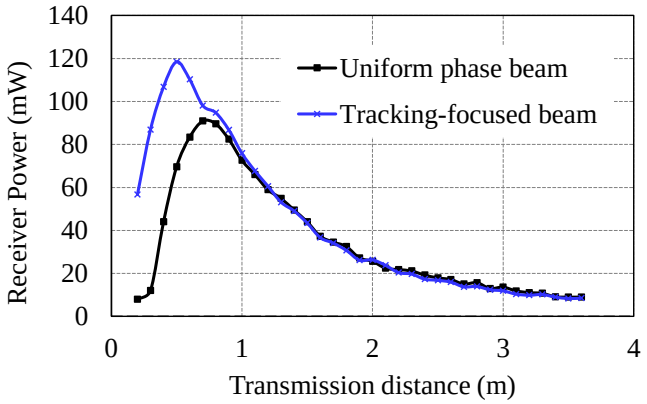

Fig. 18 Result of the beam transmission efficiency with distance.

V. Conclusion

We designed and demonstrated an image recognition-based auto-tracking WPT system using a 1 × 4 phased array. Compared to a uniform beam, an auto-tracking focused beam can significantly improve the transmission power within a ±10° angle and at a close distance. Furthermore, a tracking beam method was introduced, and the optimization beam adjusting on the distance of the receiving antenna was investigated further.

The proposed approach identified the target distance by the target projection sizes in the image recognition module. The distance identified error will caused by target projection sizes such as the angle changes. We will improve the approach of the distance identified so as to be suitable for more applications in the future. The system described in this paper implements the phase control only on the *X*-axis. we will continue to expand phased arrays on the *X*-axis and *Y*-axis to achieve a higher WPT transmission efficiency. The designed system complies with Japan WPT regulations, with the highly mature development of image recognition technology and beam tracking technology, WPT technology is expected to be more widely used.

References

[1] S. Y. Hui, "Planar Wireless Charging Technology for Portable Electronic Products and Qi," in *Proceedings of the IEEE*, vol. 101, no. 6, pp. 1290-1301, June 2013, doi:10.1109/JPROC.2013.2246531.

[2] D. van Wageningen and T. Staring, "The Qi wireless power standard," *Proceedings of 14th International Power Electronics and Motion Control Conference* EPE-PEMC 2010, 2010, pp. S15-25-S15-32.

[3] E. Strommer, M. Jurvansuu, T. Tuikka, A. Ylisaukko-oja, H. Rapakko and J. Vesterinen, "NFC-Enabled Wireless Charging," 2012 4*th International Workshop on Near Field Communication*, 2012, pp. 36-41.

[4] M. Sallinen, E. Strömmer and A. Ylisaukko-oja, "Application Scenario for NFC: Mobile Tool for Industrial Worker," 2008 *Second International Conference on Sensor Technologies and Applications (sensorcomm 2008)*, 2008, pp. 586-591.

[5] B. Nath, F. Reynolds and R. Want, "RFID Technology and Applications," in *IEEE Pervasive Computing*, vol. 5, no. 1, pp. 22-24, Jan.-March 2006, doi: 10.1109/MPRV.2006.13.

[6] R. Want, "An introduction to RFID technology," in *IEEE Pervasive Computing*, vol. 5, no. 1, pp. 25-33, Jan.-March 2006.

[7] C. T. Rodenbeck et al., "Terrestrial Microwave Power Beaming," in IEEE Journal of Microwaves, vol. 2, no. 1, pp. 28-43, Jan. 2022, doi: 10.1109/JMW.2021.3130765.

[8] J. Li, F. Yin, L. Wang, B. Cui and D. Yang, "Electromagnetic Induction Position Sensor Applied to Anti-Misalignment Wireless Charging for UAVs," in *IEEE Sensors Journal*, vol. 20, no. 1, pp. 515-524, 1 Jan.1, 2020, doi: 10.1109/JSEN.2019.2940925.

[9] Kurs, A., Karalis. A., Moffatt, R., Joannopoulos, J. D., Fisher, P., and Soljacic. M. "Wireless power transfer via strongly coupled magnetic resonances". *science*, vol. 317, no. 5834, pp. 83-86, 2007, doi:10.1126/science.1143254.

[10] Ministry of Internal Affairs and Communications, Establishing Conditions for Wireless Stations for Wireless Power Transmission (General Affairs 163), [Online]. Available: https://kanpou.npb.go.jp/20220526/20220526g00112/20220526g00112000f.html.
[Accessed: 10- June- 2022]

[11] N. Shinohara, "History and Innovation of Wireless Power Transfer via Microwaves," in IEEE Journal of Microwaves, vol. 1, no. 1, pp. 218-228, Jan. 2021, doi: 10.1109/JMW.2020.3030896.

[12] M. P. Ananda, H. Bernstein, K. E. Cunningham, W. A. Feess and E. G. Stroud, "Global Positioning System (GPS) autonomous navigation," *IEEE Symposium on Position Location and Navigation.* A Decade of Excellence in the Navigation Sciences, 1990, pp. 497-508.

[13] M. Chiani, A. Giorgetti and E. Paolini, "Sensor Radar for Object Tracking," in Proceedings of the IEEE, vol. 106, no. 6, pp. 1022-1041, June 2018, doi: 10.1109/JPROC.2018.2819697.

[14] C. Ma, B. Wu, S. Poslad and D. R. Selviah, "Wi-Fi RTT Ranging Performance Characterization and Positioning System Design," in *IEEE Transactions on Mobile Computing*, vol. 21, no. 2, pp. 740-756, 1 Feb. 2022, doi: 10.1109/TMC.2020.3012563.

[15] G. Schroeer, "A Real-Time UWB Multi-Channel Indoor Positioning System for Industrial Scenarios," 2018 International Conference on Indoor Positioning and Indoor Navigation (IPIN), 2018, pp. 1-5, doi: 10.1109/IPIN.2018.8533792.

[16] P. Spachos and K. N. Plataniotis, "BLE Beacons for Indoor Positioning at an Interactive IoT-Based Smart Museum," in IEEE Systems Journal, vol. 14, no. 3, pp. 3483-3493, Sept. 2020, doi: 10.1109/JSYST.2020.2969088.

[17] F. Wen, J. Kulmer, K. Witrisal and H. Wymeersch, "5G Positioning and Mapping With Diffuse Multipath," in IEEE Transactions on Wireless Communications, vol. 20, no. 2, pp. 1164-1174, Feb. 2021, doi: 10.1109/TWC.2020.3031180.

[18] Zichen Huang, Tsay L.W. Jacky, Xunyue Zhao, Hiroki Fukuda, Tomoo Shiigi, Hiroaki Nakanishi, Tetsuhito Suzuki, Yuichi Ogawa, Naoshi Kondo, "Position and orientation measurement system using spread spectrum sound for greenhouse robots," Biosystems Engineering, vol. 198, pp 50-62, 2020

[19] Lund-Hansen, L. C., Juul, T., Eskildsen, T. D., Hawes, I., Sorrell, B., Melvad, C., & Hancke, K. "A low-cost remotely operated vehicle (ROV) with an optical positioning system for under-ice measurements and sampling," *Cold Regions Science and Technology*, vol. 151, pp. 148-155, 2018.

[20] L. Batistić and M. Tomic, "Overview of indoor positioning system technologies," *2018 41st International Convention on Information and Communication Technology, Electronics and Microelectronics* (MIPRO), 2018, pp. 0473-0478, doi: 10.23919/MIPRO.2018.8400090.

[21] C. T. Rodenbeck et al., "Microwave and Millimeter Wave Power Beaming," in IEEE Journal of Microwaves, vol. 1, no. 1, pp. 229-259, Jan. 2021, doi: 10.1109/JMW.2020.3033992.

[22] Mitani, T., Kawashima, S., and Shinohara, N. Experimental study on a retrodirective system utilizing harmonic reradiation from rectenna. IEICE Transactions on Electronics, vol. E102.C, no. 10, pp.666-672, 2019, doi:10.1587/transele.2019MMP0004.

[23] D. Belo, D. C. Ribeiro, P. Pinho and N. Borges Carvalho, "A Selective, Tracking, and Power Adaptive Far-Field Wireless Power Transfer System," in IEEE Transactions on Microwave Theory and Techniques, vol. 67, no. 9, pp. 3856-3866, Sept. 2019, doi: 10.1109/TMTT.2019.2913653.

[24] N. Shinohara, "Beam Control Technologies With a High-Efficiency Phased Array for Microwave Power Transmission in Japan," in Proceedings of the IEEE, vol. 101, no. 6, pp. 1448-1463, Jun. 2013, doi: 10.1109/JPROC.2013.2253062.

Bo Yang (S'16–M'20) received the BE degree in electronic information engineering from China University of Petroleum, Qingdao, China in 2008, the ME and PhD degrees in electrical engineering from Kyoto University, Japan in 2018 and 2020. From 2019 to 2021, he conducted research on high power wireless power transfer systems, supported by Research Fellowships for Young Scientists sponsored by the Japan Society for the Promotion of Science (JSPS). He is currently researching high power microwave wireless power transmission at the Research Institute for Sustainable Humanosphere, Kyoto University. From 2008 to 2015, he was an RF engineer with the DAIHEN Group, Qingdao.

Tomohiko Mitani (M'05) received the B.E. degree in electrical and electronic engineering, M.E. degree in informatics, and Ph.D. degree in electrical engineering from Kyoto University, Kyoto, Japan, in 1999, 2001, and 2006, respectively. In 2003, he was an Assistant Professor with the Radio Science Center for Space and Atmosphere, Kyoto University. Since 2012, he has been an Associate Professor with the Research Institute for Sustainable Humanosphere, Kyoto University. His current research interests include the experimental study of magnetrons, microwave power transmission systems, and applied microwave engineering. Dr. Mitani is a member of the Institute of Electronics, Information and Communication Engineers (IEICE) and the Japan Society of Electromagnetic Wave Energy Applications (JEMEA). He has been a board member of JEMEA since 2015. He has been the treasurer of IEEE MTT-S Kansai Chapter since 2014.

Naoki Shinohara (M'06–SM'19) received the B.E. degree in electronic engineering, the M.E. and Ph.D (Eng.) degrees in electrical engineering from Kyoto University, Japan, in 1991, 1993 and 1996, respectively. He was a research associate in the Radio Atmospheric Science Center, Kyoto University from 1996. He was a research associate of the Radio Science Center for Space and Atmosphere, Kyoto University by recognizing the Radio Atmospheric Science Center from 2000, and there he was an associate professor since 2001. He was an associate professor in Research Institute for Sustainable Humanosphere, Kyoto University by recognizing the Radio Science Center for Space and Atmosphere since 2004. From 2010, he has been a professor in Research Institute for Sustainable Humanosphere, Kyoto University. He has been engaged in research on Solar Power Station/Satellite and Microwave Power Transmission system. He is IEEE Distinguish Microwave lecturer, IEEE MTT-S Technical Committee 26 (Wireless Power Transfer and Conversion) vice chair, IEEE MTT-S Kansai Chapter TPC member, IEEE Wireless Power Transfer Conference advisory committee member, international journal of Wireless Power Transfer (Cambridge Press) executive editor, Radio Science for URSI Japanese committee C member, past technical committee chair on IEICE Wireless Power Transfer, Japan Society of Electromagnetic Wave Energy Applications vice chair, Wireless Power Transfer Consortium for Practical Applications (WiPoT) chair, and Wireless Power Management Consortium (WPMc) chair.